crystals

MDPI

Article

Dielectric Response of $KTaO_3$ Single Crystals Weakly Co-Doped with Li and Mn

Alexander Tkach [1,*], Sebastian Zlotnik [2] and Paula M. Vilarinho [1]

[1] Department of Materials and Ceramic Engineering, CICECO–Aveiro Institute of Materials, University of Aveiro, 3810-193 Aveiro, Portugal; paula.vilarinho@ua.pt
[2] Institute of Applied Physics, Military University of Technology, 2 Kaliskiego Str., 00-908 Warsaw, Poland; sebastian.zlotnik@wat.edu.pl
* Correspondence: atkach@ua.pt

Abstract: Alkali tantalates are encouraging functional materials with versatile properties that make them potential players in microelectronics, photocatalytic processes or medicine. Here, $KTaO_3$ single crystals with 0.27% Li and 0.15% or 0.31% Mn contents determined by inductively coupled plasma spectroscopy analysis are studied at low temperatures using dielectric spectroscopy in a frequency range of 10^2–10^6 Hz. Both Li and Mn doping are found to induce separate low-frequency dielectric relaxations of comparable strength in $KTaO_3$. The relaxation dynamics follow the Arrhenius law with activation energy values of ~77 and 107 meV, attributing the relaxation origin to the dipoles formed by off-centre $Li^{+}{}_{K}$ and $Mn^{2+}{}_{K}$ ions, respectively.

Keywords: perovskites; polar dielectrics; co-doping; dielectric relaxation

check for updates

Citation: Tkach, A.; Zlotnik, S.; Vilarinho, P.M. Dielectric Response of $KTaO_3$ Single Crystals Weakly Co-Doped with Li and Mn. *Crystals* **2021**, *11*, 1222. https://doi.org/10.3390/cryst11101222

Academic Editor: Jan Macutkevic

Received: 23 September 2021
Accepted: 7 October 2021
Published: 10 October 2021

1. Introduction

Alkali tantalates, such as $KTaO_3$ (KT) and $LiTaO_3$, are members of the ferroic family of lead-free compounds with potential applications for electronic components and tissue engineering, respectively [1]. Their solid solution $K_{1-x}Li_xTaO_3$ has also been particularly intensively studied, wherein displacements of small Li ions on K sites generate strong local dipole moments, which couple electrostatically to the KT polar soft mode [2,3]. As a result, both dielectric relaxations and ferroelectric phase transition were reported for heavily Li-doped KT. For $K_{1-x}Li_xTaO_3$ systems with $x < 0.008$ [4], however, no phase transition but only relaxation was reported [2–10]. The dielectric relaxation was also reported in weakly (0.01–0.3%) Mn-doped $KTaO_3$ single crystals [11–13]. By analogy to Li-doped KT, the origin of the relaxation was shown to be the off-centre displacement of dopant ions on the K site in one of the six <001>-type crystal directions [2,3,12]. In addition to the majority of the results obtained on single crystals, low-frequency dielectric relaxations were further observed for Li- or Mn-doped KT ceramics [8,14–16]. However, in contrast to $K_{0.98}Li_{0.02}TaO_3$ ceramics [9], no ferroelectric phase transition was detected in polycrystalline $K_{0.985}Mn_{0.015}TaO_{3\pm\delta}$ [16]. Moreover, the low-temperature dielectric relaxation strength or permittivity amplitude in Li-doped KT was reported to be enhanced by weak Cu [5] or Ca donor co-doping [17], respectively, while the ferroelectric order and dipole-glass phase were reported to coexist in 1.2% Nb and 0.14% Li co-doped KT single crystals [18].

However, to the authors' best knowledge, no research on the dielectric response has been undertaken for Li and Mn co-doped $KTaO_3$. Therefore, the effect of Li and Mn co-doping on the dielectric properties of KT single crystals is addressed in this work. The dielectric permittivity of KT single crystals with 0.27% Li and 0.15% or 0.31% Mn is explored as a function of temperature and frequency and compared with a reference single 0.73% Li-doped KT crystal.

2. Materials and Methods

The crystals were grown by the self-flux solution method with conditions similar to reported elsewhere for undoped $KTaO_3$ [19]. First, for Li doping, the Li_2CO_3 precursor was used to prepare the reference Li-doped KT single crystal. Then, MnO_2 was used for Mn doping. For the dielectric measurements, gold electrodes were sputtered on major parallel faces of naturally shaped polished crystals. Complex dielectric permittivity, consisting of real part ε' and imaginary part ε'', as well as the dissipation factor tanδ = $\varepsilon''/\varepsilon'$, were measured in the frequency f range of 10^2–10^6 Hz on heating after cooling down to temperature T of 16 K using a precision LCR-meter (HP 4284A, Hewlett Packard, Palo Alto, CA, USA). A He closed-cycle cryogenic system (Displex APD-Cryostat HC-2, Allentown, PA, USA) equipped with silicon diode temperature sensors and a digital temperature controller, Scientific Instruments Model 9650, was used for T variation.

3. Results and Discussion

The ultimate concentration of the dopants in the crystals was determined by inductively coupled plasma spectroscopy (ICPS) analysis, as presented in Table 1. Accordingly, we have got two Li and Mn co-doped crystals with Mn contents of 0.15% or 0.31% and a constant Li content of 0.27% as well as the reference single Li-doped KT crystal with Li content of 0.73%. All the dopant contents are below 0.8%, which according to literature, should not result in any ferroelectric phase transition but should induce dielectric relaxations [2–4]. At the same time, in spite of a large number of literature reports on Li-doped KT crystals [2–10], the real molar Li content in the crystals is rarely determined [6]; instead, it is often just estimated to be 35% of the Li molar concentration in the melt [7,10,17,18] based on the empirical relationship reported by van der Klink and Rytz [20]. However, in the case of our reference Li-doped KT crystal, the ultimate Li content was found to be just about 15% of the Li concentration in the melt, thus likely being dependent on the crystal growth conditions. Concerning the relation between the nominal melt concentration and ultimate crystal content of Mn in KT, our ICPS analysis indicates it to be about 10%. An order of magnitude decrease in the dopant concentrations during the crystal growth was also reported for Co, Mn, Cu and Fe elements in KT crystals, although without any specifications for each element as well as for the chemical analysis kind [21].

Table 1. Li and Mn contents in $KTaO_3$ single crystals according to ICPS analysis as well as the Arrhenius law relaxation time at infinite temperatures τ_0 and activation energy U for dielectric relaxations observed on them.

ICPS Results		**Arrhenius Law**			
		Relaxation I		**Relaxation II**	
Li content (%)	**Mn Content (%)**	τ_0 **(s)**	U **(meV)**	τ_0 **(s)**	U **(meV)**
0.27(3)	0.15(2)	$1.16(15) \times 10^{-13}$	79.18(55)	$1.41(29) \times 10^{-14}$	108.83(99)
0.27(3)	0.31(3)	$1.68(26) \times 10^{-13}$	77.18(69)	$2.95(37) \times 10^{-14}$	105.34(68)

$\varepsilon'(T)$ of the reference Li-doped KT single crystal shown in Figure 1a reveals a dielectric relaxation reflected by a diffuse peak, where the amplitude and position depend on the frequency (see Appendix A Figure A1) in contrast to undoped $KTaO_3$, revealing no frequency dispersion and a continuous increase in the dielectric permittivity with decreasing temperatures [19] in accordance with the incipient ferroelectric behaviour. As shown in Figure 1b,1c, this relaxation (I) is also seen in both $\varepsilon''(T)$ and $tan\delta(T)$ of Li-doped $KTaO_3$ with the peak temperatures of about 50 K at 17 kHz. Co-doping with Mn is found to induce an additional peak in temperature dependences of both the dielectric permittivity and dissipation factor at about 62 K, as shown in Figure 1 and marked as relaxation II. The relaxation II peak amplitude increases with the increasing Mn content. Thus, we can clearly associate relaxation I with Li doping and relaxation II with Mn doping.

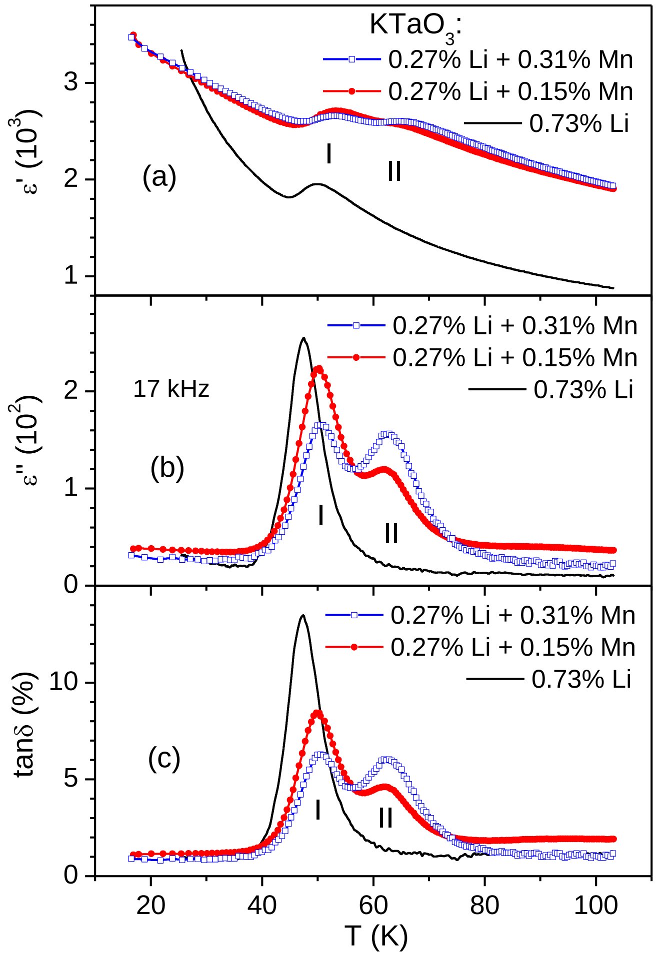

Figure 1. Real ε' (**a**) and imaginary ε'' (**b**) parts of the dielectric permittivity and dissipation factor tanδ (**c**) of $KTaO_3$: 0.73% Li (solid line), $KTaO_3$: 0.27% Li and 0.15% Mn (open squares) and $KTaO_3$: 0.27% Li and 0.31% Mn (solid circles) single crystals as a function of temperature T at about 17 kHz.

The observed dielectric response has differences comparing with that for other co-doped KT crystals [5,17,18]. In contrast to the enhancement of Li-induced relaxation by Cu co-doping [5], we have observed that Mn co-doping induces independent relaxation instead. There is a kind of similarity with Li and Ca co-doped KT crystals, where not only the dielectric permittivity peak but also the permittivity level in a presented temperature range of 4–200 K was found to be raised by about an order of magnitude by donor Ca^{2+} co-doping on the K^+ site [17]. However, in our case, Mn^{2+} co-doping on the K^+ site [12,16] only enhances the permittivity level about twice at 100 K and does not raise it below 27 K, inducing independent relaxation once again in contrast to Ca co-doping. In the case of Nb and Li co-doped KT crystals, the ferroelectric phase transition was induced by Nb at a temperature below that of the Li-induced relaxation, enhancing the relaxation intensity as well [18]. In our crystals, however, there was not a lower temperature phase transition but higher temperature relaxation induced by Mn co-doping without an evident effect on the Li-induced relaxation strength.

Figure 2 illustrates the dielectric response evolution for Li and Mn co-doped KT crystals with the frequency. The relaxation I peak temperature in $\varepsilon''(T)$ dependence varies from about 42 K at 500–700 Hz to about 65 K at 1 MHz for both $KTaO_3$: 0.27% Li + 0.15% Mn (Figure 2a) and $KTaO_3$: 0.27% Li + 0.31% Mn (Figure 2b) single crystals. At frequencies below 500–700 Hz, the dielectric response obtained using our setup becomes too noisy for proper analysis. The relaxation II peak temperature varies from about 53 K at 500 Hz to about 70 K at 200 kHz for $KTaO_3$: 0.27% Li + 0.15% Mn (Figure 2a) and from about 54 K at 700 Hz to about 79 K at 1 MHz for $KTaO_3$: 0.27% Li + 0.31% Mn (Figure 2b) crystals. For

0.15% Mn content, the relaxation II becomes too weak and is thereby hidden by relaxation I above a frequency of 200 kHz to determine its peak temperature well.

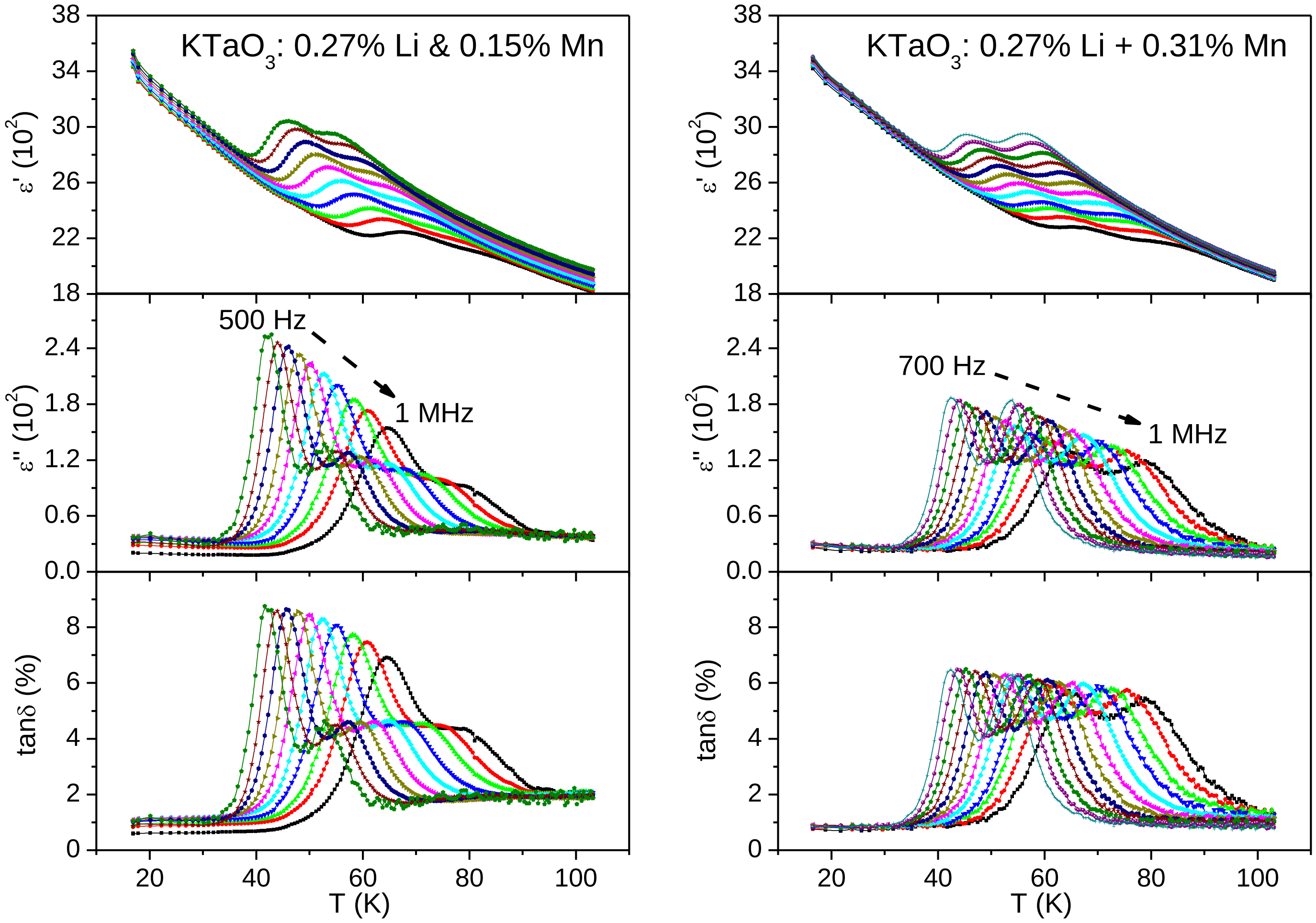

(**a**) (**b**)

Figure 2. Real ε' (**top panels**) and imaginary ε'' (**middle panels**) parts of the dielectric permittivity and dissipation factor tanδ (**bottom panels**) of KTaO$_3$: 0.27% Li + 0.15% Mn (**a**) and KTaO$_3$: 0.27% Li + 0.31% Mn (**b**) single crystals as a function of temperature T at different frequencies from 500 Hz to 1 MHz.

Concerning the $\varepsilon''(T)$ peak intensity, it is evidently higher for relaxation I in KTaO$_3$: 0.27% Li + 0.15% Mn crystal compared to that of relaxation II (Figure 2a). However, the increase in Mn content to 0.31% also raises the relaxation II peak intensity, thus confirming their relation once again. Moreover, for KTaO$_3$: 0.27% Li + 0.31% Mn crystal with very close Li and Mn contents, the $\varepsilon''(T)$ peak intensity is also very similar, particularly in the low-frequency range (Figure 2b). Just at high frequencies, the intensity of relaxation II peak becomes lower than that of relaxation I.

Using the $\varepsilon''(T)$ peak temperature values at corresponding frequencies, an analysis of the dielectric relaxation dynamics was carried out assuming the Debye approximation. Accordingly, the set of independent dipoles is characterized by a unique relaxation time (τ), which is equal to the inverse of the angular relaxation frequency ($\omega = 2\pi f$). Then the relaxation is described by the Arrhenius law:

$$\tau = \tau_0 \exp(U/k_B T), \quad (1)$$

where τ_0 is the relaxation time at infinite temperatures; U is the activation energy of the dipolar process; k_B is the Boltzmann constant; T is the absolute temperature. The dynamics of the diffuse peaks were examined using Arrhenius plots ln(τ) vs $1000/T_{\varepsilon''m}$ ($T_{\varepsilon''m}$ stands for the temperature at which the maximum of ε'' occurs at the angular frequency $w = 2\pi f = \tau^{-1}$), as presented in Figure 3. The activation energies U are found to be 77–79 and 105–109 meV and pre-exponential term τ_0 is 116–168 and 14–30 fs for relaxations I and II, respectively, as presented in Table 1. A smaller ionic size and larger off-centre displacement of Li^+ ions compared to Mn^{2+} ones should be responsible for lower relaxation activation energy and a larger relaxation time.

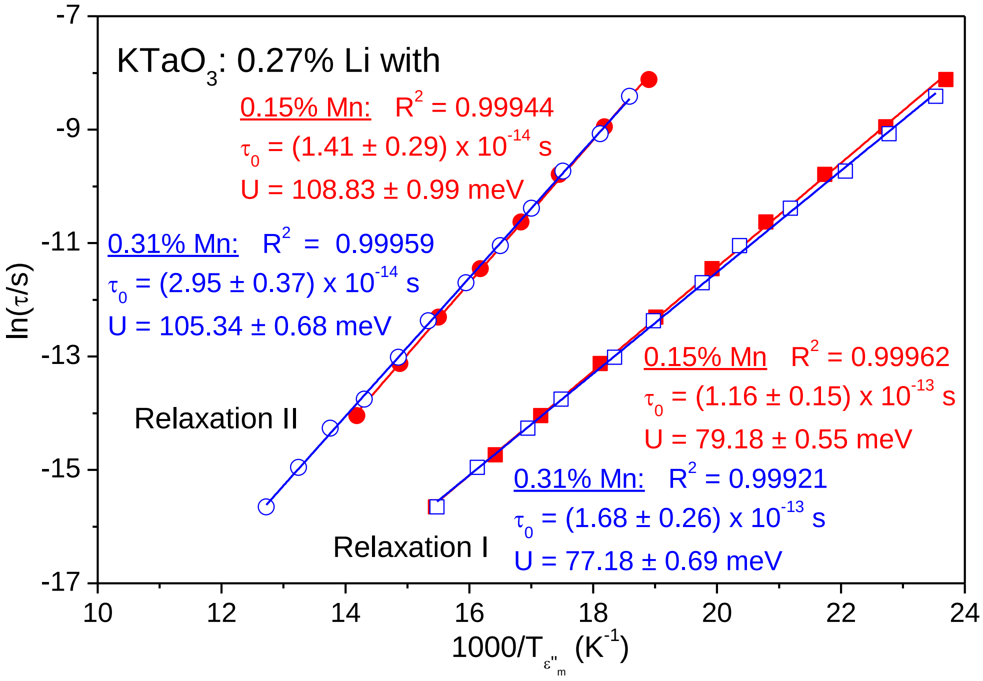

Figure 3. Arrhenius plot ln(τ) versus $1000/T_{\varepsilon''m}$ for the dielectric relaxations I (squares) and II (circles) of $KTaO_3$: 0.27% Li + 0.15% Mn (solid symbols) and $KTaO_3$: 0.27% Li + 0.31% Mn (open symbols) single crystals with fits to the Arrhenius law (solid lines) and the fit parameters.

The Arrhenius law parameters for relaxation II of Li and Mn co-doped KT single crystals presented in Table 1 are very close to the U = 104–110 meV and τ_0 = 5–20 fs values obtained on 0.01–0.3% Mn-doped $KTaO_3$ crystals using dielectric spectroscopy and electron spin resonance analysis [11,12], as shown in Table 2. The values of 105 meV and 46 fs reported for single-phase 1.5% Mn-doped KT ceramics [16] are also rather close. The origin of relaxation II observed in Li and Mn co-doped KT crystals with the activation energy of ~107 meV can thus be attributed to the displacement of Mn^{2+} from the centre of the K^+ site in one of the six <001>-type directions, as reported for Mn-doped $KTaO_3$ single crystals [12].

Table 2. Arrhenius law parameters for the dielectric relaxation dynamics in weakly (≤1%) Li- or Mn-doped as well as co-doped $KTaO_3$ single crystals.

Composition	Arrhenius Law		Ref.
	τ_0 (fs)	U (meV)	
KT: (0.01–0.1%) Mn	20	105–110	Nowick et al., 1994 [11]
KT: (0.01–0.3%) Mn	5–20	104–110	Laguta et al., 2000 [12]
KT: (0.01–0.3%) Mn	83–200	93–98	Venturini et al., 2005 [13]
KT: 1% Li	-	55–79	Doussineau et al., 1993 [22]
KT: 0.9% Li	13	86	Borsa et al., 1980 [23]
KT: 0.6% Li	135	78	Prosandeev et al., 2001 [6]
KT: 0.18% Li	-	78	Trybula et al., 2012 [10]
KT: 0.18% Li	22–57	82–84	Dec et al., 2005 [7]
KT: (0.1–1.0)% Li	60–67	82–84	Trepakov et al., 1999 [5]
KT: 0.1% Li + 0.02 wt.% Cu	33	81	
KT: 0.5% Li + 0.1 wt.% Fe	45	84	
KT: 0.6% Li + 0.03 wt.% Cu	33	81	
KT: 0.14% Li + 1.2% Nb	30	89	Trepakov et al., 2001 [18]
KT: 5% Li + 0.0015% Ca	240	79	Wakimoto et al., 2006 [17]

The relaxation parameters for Li weakly (≤ 1%) doped and co-doped KT single crystals reported in literature, mainly using the dielectric spectroscopy technique [5–7,10,17,18,22] sometimes accompanied by nuclear magnetic resonance [23], are also listed in Table 2. They are closer to the relaxation I parameters presented in Table 1 for Li and Mn co-doped KT single crystals. The closest U of 78–79 meV and τ_0 of 135–240 fs values are those reported for KT: 0.18% Li [10] and KT: 0.6% Li [6] crystals as well as for KT: 1% Li [22] and one of the relaxations of 5% Li + 0.0015% Ca co-doped KT crystal [17]. One of the relaxations of 2–10% Li-doped KT ceramics has parameters of 76–78 meV and 11–270 fs as well [8]. Thus, the relaxation I with the activation energy of ~78 meV evidently originates from the reorientation of Li^+ between equivalent positions on K^+ sites of KT crystals [2].

4. Conclusions

$KTaO_3$ single crystals with 0.27% Li and 0.15% or 0.31% Mn contents determined by ICPS analysis were grown by the self-flux solution method. Their dielectric spectroscopy characterisation at temperatures between 16 and 104 K in a frequency range of 10^2–10^6 Hz showed two pronounced dielectric relaxations in contrast to other co-doped $KTaO_3$ single crystals. The Arrhenius law parameters U~78 and 107 meV, as well as τ_0~142 and 22 fs, were found for these relaxations, helping to attribute them to the formation of polar regions by the introduction and off-centre displacements of Li^+ and Mn^{2+} on the K^+ site, respectively.

Author Contributions: Conceptualisation, P.M.V. and A.T.; methodology, S.Z.; validation, S.Z.; formal analysis, A.T.; investigation, S.Z. and A.T.; resources, P.M.V.; data curation, S.Z.; writing—original draft preparation, A.T.; writing—review and editing, S.Z.; visualisation, A.T.; supervision, P.M.V.; project administration, P.M.V.; funding acquisition, P.M.V. All authors have read and agreed to the published version of the manuscript.

Funding: This work was developed within the scope of the project CICECO-Aveiro Institute of Materials, UIDB/50011/2020 & UIDP/50011/2020, financed by national funds through the Portuguese Foundation for Science and Technology/MCTES.

Data Availability Statement: The data presented in this study are available on request from the corresponding author.

Conflicts of Interest: The authors declare no conflict of interest.

Appendix A

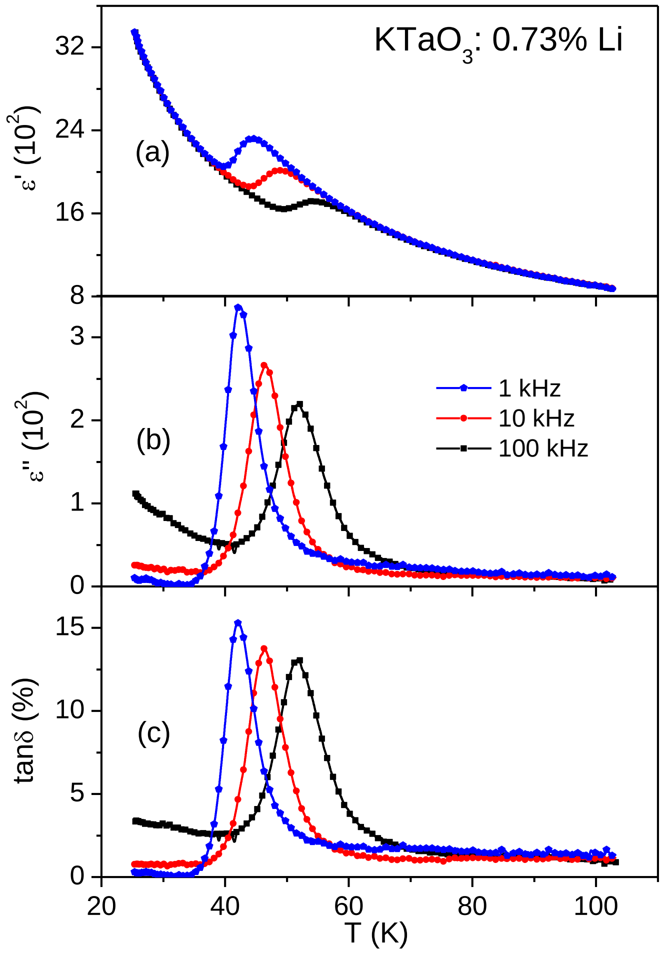

Figure A1. Real ε' (**a**) and imaginary ε'' (**b**) parts of the dielectric permittivity and dissipation factor tanδ (**c**) of $KTaO_3$: 0.73% Li single crystals as a function of temperature T at 1 (pentagon), 10 (circle) and 100 (square) kHz.

References

1. Zlotnik, S.; Tkach, A.; Vilarinho, P.M. Functional tantalum based oxides: From the structure to the applications. In *Advanced Ceramic Materials*; Tiwari, A., Gerhardt, R.A., Szutkowska, M., Eds.; WILEY-Scrivener Publishing LLC: USA, 2016; pp. 337–383.
2. Samara, G.A. The relaxational properties of compositionally disordered ABO_3 perovskites. *J. Phys. Condens. Matter* **2003**, *15*, R367–R411. [CrossRef]
3. Vugmeister, B.E.; Glinchuk, M.D. Dipole glass and ferroelectricity in random-site electric dipole systems. *Rev. Mod. Phys.* **1990**, *62*, 993–1026. [CrossRef]
4. Geifman, I.N. Phase transitions in $K_{1\text{-}x}Li_xTaO_3$. *Ferroelectrics* **1992**, *131*, 207–212. [CrossRef]
5. Trepakov, V.; Vikhnin, V.; Savinov, M.; Syrnikov, P.; Kapphan, S.; Lemanov, V.; Hesse, H.; Jastrabik, L. Dielectric permittivity and Fe-and Cu-doping effect in $KTaO_3$ and $K_{1\text{-}x}Li_xTaO_3$. *Ferroelectrics* **1999**, *235*, 59–75. [CrossRef]
6. Prosandeev, S.A.; Trepakov, V.A.; Savinov, M.E.; Kapphan, S.E. Coupling of Li+ relaxators to the soft mode in $KTaO_3$:Li. *J. Phys. Condens. Matter* **2001**, *13*, 719–725. [CrossRef]
7. Dec, J.; Miga, S.; Trybula, Z.; Kaszynska, K.; Kleemann, W. Dynamics of Li+ dipoles at very low concentration in quantum paraelectric potassium tantalite. *J. Appl. Phys.* **2010**, *107*, 094102. [CrossRef]
8. Tkach, A.; Almeida, A.; Agostinho Moreira, J.; Espinha, A.; Chaves, M.R.; Perez de la Cruz, J.; Vilarinho, P.M. Lithium-induced dielectric relaxations in potassium tantalate ceramics. *J. Phys. D Appl. Phys.* **2011**, *44*, 315406. [CrossRef]
9. Tkach, A.; Almeida, A.; Agostinho Moreira, J.; Chaves, M.R.; Espinha, A.; Vilarinho, P.M. Polar behaviour induced by lithium in potassium tantalate ceramics. *J. Phys. Condens. Matter* **2012**, *24*, 045906. [CrossRef]
10. Trybula, Z.; Los, S.; Trybula, M.; Kaszynska, K.; Dec, J.; Miga, S.; Laguta, V.V. $K_{0.9982}Li_{0.0018}TaO_3$ crystal under external DC electric field. *Ferroelectrics* **2012**, *428*, 36–42. [CrossRef]

11. Nowick, A.S.; Fu, S.Q.; Lee, W.-K.; Lim, B.S.; Scherban, T. Dielectric relaxation of paired defects in perovskite-type oxides. *Mater. Sci. Eng. B* **1994**, *23*, 19–24. [CrossRef]
12. Laguta, V.V.; Glinchuk, M.D.; Bykov, I.P.; Rosa, J.; Jastrabik, L.; Savinov, M.; Trybuła, Z. Paramagnetic dipole centers in $KTaO_3$: Electron-spin-resonance and dielectric spectroscopy study. *Phys. Rev. B* **2000**, *61*, 3897–3904. [CrossRef]
13. Venturini, E.L.; Samara, G.A.; Laguta, V.V.; Glinchuk, M.D.; Kondova, I.V. Dipolar centers in incipient ferroelectrics: Mn and Fe in $KTaO_3$. *Phys. Rev. B* **2005**, *71*, 094111. [CrossRef]
14. Shvartsman, V.V.; Bedanta, S.; Borisov, P.; Kleemann, W.; Tkach, A.; Vilarinho, P.M. Spin cluster glass and magnetoelectricity in Mn-doped $KTaO_3$. *J. Appl. Phys.* **2010**, *107*, 103926. [CrossRef]
15. Axelsson, A.-K.; Pan, Y.; Valant, M.; Vilarinho, P.M.; Alford, N.M. Polar fluctuations in Mn substituted $KTaO_3$ ceramics. *J. Appl. Phys.* **2010**, *108*, 064109. [CrossRef]
16. Tkach, A.; Almeida, A.; Levin, I.; Woicik, J.C.; Vilarinho, P.M. Dielectric relaxation, local structure and lattice dynamics in Mn-doped potassium tantalate ceramics. *Materials* **2021**, *14*, 4632. [CrossRef]
17. Wakimoto, S.; Samara, G.A.; Grubbs, R.K.; Venturini, E.L.; Boatner, L.; Xu, A.G.; Shirane, G.; Lee, S.-H. Dielectric properties and lattice dynamics of Ca-doped $K_{0.95}Li_{0.05}TaO_3$. *Phys. Rev. B* **2006**, *74*, 054101. [CrossRef]
18. Trepakov, V.A.; Savinov, M.E.; Kapphan, S.E.; Giulotto, E.; Galinetto, P.; Camagni, P.; Samoggia, G.; Boatner, L.A. Dipole ordering effects and reentrant dipolar glass state in $KTaO_3$:Li,Nb. *Phys. Rev. B* **2001**, *63*, 172203. [CrossRef]
19. Zlotnik, S.; Vilarinho, P.M.; Costa, M.E.V.; Moreira, J.A.; Almeida, A. Growth of incipient ferroelectric $KTaO_3$ single crystals by a modified self-flux solution method. *Cryst. Growth Des.* **2010**, *10*, 3397–3404. [CrossRef]
20. Van Der Klink, J.J.; Rytz, D. Growth of $K_{1\text{-}x}Li_xTaO_3$ crystals by a slow-cooling method. *J. Cryst. Growth* **1982**, *56*, 673–676. [CrossRef]
21. Fu, S.Q.; Lee, W.-K.; Nowick, A.S.; Boatner, L.A.; Abraham, M.M. Study of protons in acceptor-doped $KTaO_3$ crystals by IR and EPR techniques. *J. Solid State Chem.* **1989**, *83*, 221–229. [CrossRef]
22. Doussineau, P.; Farssi, Y.; Frénois, C.; Levelut, A.; McEnaney, K.; Toulouse, J.; Ziolkiewicz, S. Strophoidal Argand diagram and the distribution of relaxation times in $K_{1\text{-}x}Li_xTaO_3$. *Phys. Rev. Lett.* **1993**, *70*, 96–99. [CrossRef] [PubMed]
23. Borsa, F.; Höchli, U.T.; Van Der Klink, J.J.; Rytz, D. Condensation of random-site electric dipoles: Li in $KTaO_3$. *Phys. Rev. Lett.* **1980**, *45*, 1884–1887. [CrossRef]